Geometric quantum gates with superconducting qubits

I. Kamleitner,[1] P. Solinas,[2] C. Müller,[1,3] A. Shnirman,[1,3] and M. Möttönen[2,4]

[1]*Institut für Theory der Kondensierten Materie, Karlsruher Institut für Technologie, 76128 Karlsruhe, Germany*

[2]*Department of Applied Physics/COMP, Aalto University, P.O. Box 14100, FI-00076 Aalto, Finland*

[3]*DFG-Center for Functional Nanostructures (CFN), D-76128 Karlsruhe, Germany*

[4]*Low Temperature Laboratory, Aalto University, P.O. Box 13500, FI-00076 Aalto, Finland*

(Received 5 April 2011; revised manuscript received 21 April 2011; published 15 June 2011)

We suggest a scheme to implement a universal set of non-Abelian geometric transformations for a single logical qubit composed of three superconducting qubits coupled to a single cavity. The scheme utilizes an adiabatic evolution in a rotating frame induced by the effective tripod Hamiltonian which is achieved by longitudinal driving of the qubits. The proposal is experimentally feasible with the current state of the art and could serve as a first proof of principle for geometric quantum computing.

DOI: 10.1103/PhysRevB.83.214518 PACS number(s): 03.65.Vf, 85.25.Cp, 03.67.Lx

I. INTRODUCTION

Superconducting qubits, also known as artificial atoms, have emerged as a promising candidate to achieve quantum computing.[1] The properties of these nanoscale systems can be designed to a large extent, and systems have been found where many logical operations can be performed within the decoherence time.[2,3] Superconducting qubits can be coupled via thin-film microwave cavities[4,5] to allow for two-qubit gates and ultimately for universal quantum computing. Furthermore, they have the intrinsic scalability of condensed matter systems and the high-precision measurement features of quantum optical systems.

Error correction theory predicts that fault tolerant quantum computing requires of the order of 10^4 quantum operations with only a single error on average.[6,7] Contrary to classical computation, where gates and errors are discrete, in quantum computation many small errors can accumulate to an eventual bit or phase flip. Therefore, enormous accuracy for single gates is required. Typically, the control parameters cannot be controlled to such precision and especially the exact timing of control pulses remains challenging. As a possible solution, holonomic quantum computing was proposed.[8] In this case, the unitary transformations depend only on the path which the control parameters trace in parameter space, but not on their timing. Furthermore, random rapidly fluctuating deviations of the actual path to the desired one cancel to the first order.[9,10] Thus, the precision of holonomic quantum gates can possibly be considerably higher than that of the precision of the control parameters itself.

Abelian holonomies, referred to as geometric phases or Berry phases, have been observed in a wide variety of systems including superconducting qubits.[11,12] The situation is quite different for non-Abelian holonomies necessary for universal geometric quantum computing. Despite several theoretical proposals,[13–18] no such adiabatic transformation has been experimentally observed in superconducting qubits or in any other systems. Here, we present a scheme for the implementation of a non-Abelian holonomy which is feasible with the devices and methods used in current experiments on transmon qubits.[2] Although our method might also work for other superconducting qubits, we choose to work with transmons because of the ability to drive purely longitudinally using flux lines and because of the long decoherence time.

Our method is based on the much studied tripod Hamiltonian

$$\hat{H} = \hbar \sum_{j=1}^{3} (\Omega_i |0\rangle\langle i| + \text{h.c.}) \hat{=} \hbar \begin{pmatrix} 0 & \Omega_1 & \Omega_2 & \Omega_3 \\ \Omega_1^* & 0 & 0 & 0 \\ \Omega_2^* & 0 & 0 & 0 \\ \Omega_3^* & 0 & 0 & 0 \end{pmatrix}, \tag{1}$$

where the $\Omega_i(t)$ are the control parameters (usually referred to as Rabi frequencies) and the matrix representation is given in the basis $\{|i\rangle\}$, $i = 0,1,2,3$. The first proposal to observe non-Abelian transformations in trapped ions was based on Hamiltonian equation (1), which is sufficient to implement an arbitrary $U(2)$ transformations between the states $|1\rangle$ and $|2\rangle$ used as the logical qubit.[19,20] Similar structures have been recovered in many quantum systems and similar implementations have been proposed,[21–24] but yet without experimental verification.

Based on recent experiments,[2] we propose a way to implement a universal set of single-qubit non-Abelian geometric transformations in a system of three superconducting transmon qubits coupled to the same cavity. Each transmon is composed of two superconducting islands connected by two Josephson junctions, thus forming a superconducting loop.[2,3] The control parameters are the magnetic fluxes through the loops of each transmon, which can be controlled individually allowing us to adiabatically drive the system along a control cycle. With realistic approximations, we are able to obtain an effective tripod Hamiltonian in a rotating frame.

The paper is organized as follows. In Sec. II, we introduce the physical setup of the proposed experiment and in Sec. III, we derive the effective tripod Hamiltonian. Section IV is devoted to numerical studies. We conclude the work in Sec. V.

II. PHYSICAL SYSTEM

The superconducting qubits considered here are commonly referred to as transmons.[3,25] Their structure is similar to a charge qubit, but they have a much larger total capacitance C_Σ such that the ratio of the charging energy $E_C = e^2/(2C_\Sigma)$ over the Josephson energy E_J is much lower than unity. This results in a small charge dispersion of the energy eigenstates, which in turn leads to a significantly reduced sensitivity to charge noise and much longer decoherence times, typically of

the order of a few microseconds. On the downside, they have a smaller anharmonicity compared with charge qubits.

Our scheme includes three qubits with frequencies $\varepsilon_i/2\pi$, $i = 1,2,3$. They are coupled to a cavity mode with frequency $\omega/2\pi$. The combined system is described by the Tavis-Cummings Hamiltonian[2,3]

$$\hat{H} = \hbar\omega\hat{a}^\dagger\hat{a} + \sum_{i=1}^{3}\left[\frac{1}{2}\hbar\varepsilon_i\hat{\sigma}_z^{(i)} + \hbar g_i(\hat{\sigma}_+^{(i)}\hat{a} + \hat{\sigma}_-^{(i)}\hat{a}^\dagger)\right], \quad (2)$$

where $g_i/2\pi$ is the qubit-cavity coupling frequency, $\hat{\sigma}^{(i)}$ are the usual Pauli operators for the ith qubit, and $\hat{a}$ and $\hat{a}^\dagger$ are the bosonic annihilation and creation operators, respectively, for the cavity mode. To arrive at the above Hamiltonian, we used the rotating wave approximation (RWA), assuming that the coupling strengths g_i are small compared with the excitation energies, which will be the case throughout the paper.

Furthermore, we neglected higher levels of the qubits which is very well justified, because we do not drive them transversally and therefore do not induce excitations to higher energy levels, and we initialize the system in the one-excitation subspace.[26] In this case, the only states involved in the dynamics are $\{|1ggg\rangle, |0egg\rangle, |0geg\rangle, |0gge\rangle\}$, where the first state in the tensor product represents the photon number in the cavity mode and the states $|e\rangle$ and $|g\rangle$ are the excited and ground states of each qubit. The Hamiltonian restricted to this subspace, written in matrix form, reads

$$H = \hbar\begin{pmatrix} 0 & g_1 & g_2 & g_3 \\ g_1 & \Delta_1 & 0 & 0 \\ g_2 & 0 & \Delta_2 & 0 \\ g_3 & 0 & 0 & \Delta_3 \end{pmatrix}, \quad (3)$$

where $\Delta_i = \varepsilon_i - \omega$ is the detuning of the ith qubit from the cavity (see Fig. 1).

The qubit frequencies ε_i, the detuning Δ_i, and the system-cavity coupling strengths g_i depend on the Josephson energy

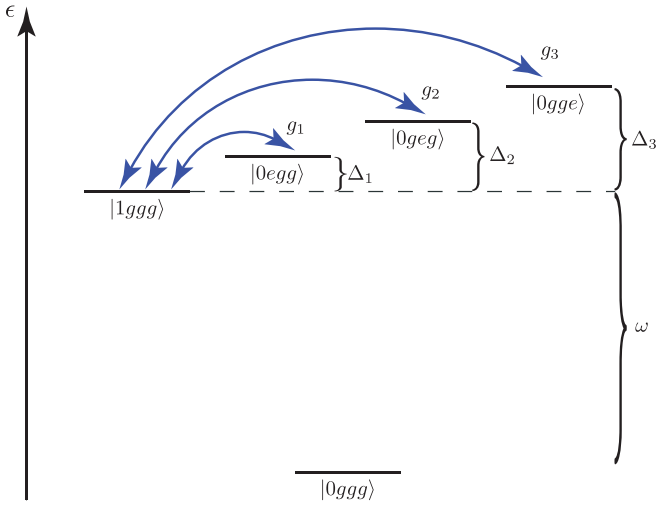

FIG. 1. (Color online) The level structures of the lowest energy states of the Hamiltonian equation (2) are shown. The photon excitation number of the cavity is labeled by $|n\rangle$, while $|g\rangle$ and $|e\rangle$ are the ground and excited states of the three qubits, respectively. The couplings between the one-excitation levels g_i are small compared to the detunings Δ_i.

$E_J^{(i)}(\phi_i)$ and thus on the controllable flux ϕ_i through the ith qubit. The Josephson energy can be written as $E_J^{(i)}(\phi_i) = E_{J\max}^{(i)}\cos(\pi\phi_i)$, where $E_{J\max}^{(i)}$ is the maximum Josephson energy and ϕ_i is in units of the flux quantum $h/(2e)$. Explicitly, we have[2,3,27]

$$\varepsilon_i(\phi_i) = \sqrt{\frac{8E_C^{(i)}E_{J\max}^{(i)}|\cos(\pi\phi_i)|}{\hbar^2}},$$
$$g_i(\phi_i) = g_{\max}^{(i)}[\cos(\pi\phi_i)]^{\frac{1}{4}}, \quad (4)$$

where $g_{\max}^{(i)}$ is a constant depending on the system parameters which can be determined experimentally.

By changing the flux $\phi_i(t)$ through the ith qubit, we can control the coupling strength $g_i(t)$ as well as the detuning $\Delta_i(t)$. We separate the dominant constant contributions [denoted with superscript (0)] which defines the properties of the nondriven system from the small time-dependent ones, which are used to drive the system. We employ the notation

$$\text{Flux:}\phi_i(t) = \phi_i^{(0)} + \delta\phi_i(t),$$
$$\text{Detuning:}\Delta_i(t) = \Delta_i^{(0)} + \delta\Delta_i(t),$$
$$\text{Coupling:}g_i(t) = g_i^{(0)} + \delta g_i(t),$$
$$\text{Hamiltonian:}H(t) = H^{(0)} + \delta H(t).$$

We assume that the flux modulation is small compared to the flux quantum, i.e., $\delta\phi_i(t) \ll 1$, and use a first-order expansion in $\delta\phi_i$ to obtain the time-dependent quantities. Because the cavity frequency is independent of the flux, we have $\delta\Delta_i = \delta\varepsilon_i$. Together with $g_i(\phi) \propto \sqrt{\varepsilon_i(\phi)}$, we obtain a useful relation between the coupling and detuning variations

$$\delta g_i(\delta\phi_i) = \frac{g_i^{(0)}\left(\phi_i^{(0)}\right)}{2\varepsilon_i^{(0)}\left(\phi_i^{(0)}\right)}\delta\Delta_i(\delta\phi_i), \quad (5)$$

which is valid up to first order in $\delta\phi_i$. Since typically $g_i^{(0)} \ll \varepsilon_i^{(0)}$, the driving via the flux has a much smaller effect on the qubit-cavity coupling g_i than on the detuning Δ_i, and therefore results mainly in longitudinal driving. However, as we will see in Sec. III, the variations in the detuning induce transitions in higher order perturbation theory, which we refer to as indirect coupling. Whether, the direct or the indirect coupling gives the leading contribution to the effective tripod Hamiltonian will turn out to depend on the ratio $\Delta_i^{(0)}/\varepsilon_i^{(0)}$.

III. EFFECTIVE TRIPOD HAMILTONIAN

In this section, we show how to obtain an effective tripod Hamiltonian from the Hamiltonian equation (3). In particular, the normal tripod approach which solely utilizes the driving of the off-diagonals of the Hamiltonian will not work for our situation, because our control over g_i is rather limited. Nevertheless, we will find that driving the diagonals results in an indirect coupling of the different eigenstates of $H^{(0)}$ which is of the desired tripod form.

To this end, we assume that the time-dependent fluxes $\delta\phi_i(t)$ oscillate with the frequencies $\omega_i/2\pi$ and we write

$$\delta\phi_i(t) = F_i(t)\cos[\omega_i t + \varphi_i(t)],$$
$$\delta\Delta_i(t) = L_i(t)\cos[\omega_i t + \varphi_i(t)], \quad (6)$$
$$\delta g_i(t) = T_i(t)\cos[\omega_i t + \varphi_i(t)],$$

where the adiabatically changing amplitudes $L_i(t)$ and $T_i(t)$ are related with the externally controllable magnitude of the flux oscillations $F_i(t)$ by Eq. (4). To realize a universal set of single-qubit transformations, also the relative phases $\varphi_i(t)$ of the oscillations need to change adiabatically in time.[20]

Anticipating that $\delta H(t)$ drives transitions between the eigenstates of $H^{(0)}$, we diagonalize $H^{(0)}$. Up to the first order in $g_i^{(0)}/\Delta_i^{(0)}$, the eigenstates of $H^{(0)}$ in the basis $\{|1ggg\rangle, |0egg\rangle, |0geg\rangle, |0gge\rangle\}$ are given by

$$v_0 \approx \begin{pmatrix} 1 \\ -g_1^{(0)}/\Delta_1^{(0)} \\ -g_2^{(0)}/\Delta_2^{(0)} \\ -g_3^{(0)}/\Delta_3^{(0)} \end{pmatrix}, \quad v_1 \approx \begin{pmatrix} g_1^{(0)}/\Delta_1^{(0)} \\ 1 \\ 0 \\ 0 \end{pmatrix}, \quad v_2 \approx \begin{pmatrix} g_2^{(0)}/\Delta_2^{(0)} \\ 0 \\ 1 \\ 0 \end{pmatrix}, \quad v_3 \approx \begin{pmatrix} g_3^{(0)}/\Delta_3^{(0)} \\ 0 \\ 0 \\ 1 \end{pmatrix}. \tag{7}$$

The Hamiltonian $H(t) = H^{(0)} + \delta H(t)$ in this basis assumes the form

$$H^D(t) = \hbar \begin{pmatrix} 0 & \delta g_1(t) - \frac{g_1^{(0)}}{\Delta_1^{(0)}}\delta\Delta_1(t) & \delta g_2(t) - \frac{g_2^{(0)}}{\Delta_2^{(0)}}\delta\Delta_2(t) & \delta g_3(t) - \frac{g_3^{(0)}}{\Delta_3^{(0)}}\delta\Delta_3(t) \\ \delta g_1(t) - \frac{g_1^{(0)}}{\Delta_1^{(0)}}\delta\Delta_1(t) & E_1 + \delta\Delta_1(t) & 0 & 0 \\ \delta g_2(t) - \frac{g_2^{(0)}}{\Delta_2^{(0)}}\delta\Delta_2(t) & 0 & E_2 + \delta\Delta_2(t) & 0 \\ \delta g_3(t) - \frac{g_3^{(0)}}{\Delta_3^{(0)}}\delta\Delta_3(t) & 0 & 0 & E_3 + \delta\Delta_3(t) \end{pmatrix},$$

where the frequencies E_i can be obtained by perturbation theory

$$E_i \approx \Delta_i^{(0)} + \frac{2\left(g_i^{(0)}\right)^2}{\Delta_i^{(0)}} + \sum_{j\neq i} \frac{\left(g_j^{(0)}\right)^2}{\Delta_j^{(0)}}. \tag{8}$$

In order to obtain the Hamiltonian equation (1), we choose $\delta g_i(t)$ and $\delta\Delta_i(t)$ to oscillate with frequency $\omega_i = E_i$. Moving into the rotating frame with respect to the diagonal dominant contribution $H^{\text{diag}} = \text{diag}\{0, E_1, E_2, E_3\}$ and using Eq. (6) we find

$$H^D(t) = \hbar \begin{pmatrix} 0 & \Omega_1\{1 + e^{-2i[\omega_1 t+\varphi_1]}\} & \Omega_2\{1 + e^{-2i[\omega_2 t+\varphi_2]}\} & \Omega_3\{1 + e^{-2i[\omega_3 t+\varphi_3]}\} \\ \Omega_1^*\{1 + e^{2i[\omega_1 t+\varphi_1]}\} & L_1\cos[\omega_1 t + \varphi_1] & 0 & 0 \\ \Omega_2^*\{1 + e^{2i[\omega_2 t+\varphi_2]}\} & 0 & L_2\cos[\omega_2 t + \varphi_2] & 0 \\ \Omega_3^*\{1 + e^{2i[\omega_3 t+\varphi_3]}\} & 0 & 0 & L_3\cos[\omega_3 t + \varphi_3] \end{pmatrix}. \tag{9}$$

Here, we defined the effective Rabi frequencies

$$\begin{aligned} \Omega_i(t) &= \left(\frac{T_i(t)}{2} - \frac{g_i^{(0)}L_i(t)}{2\Delta_i^{(0)}}\right) e^{i\varphi_i} \\ &= L_i(t)\left(\frac{g_i^{(0)}}{4\varepsilon_i^{(0)}} - \frac{g_i^{(0)}}{2\Delta_i^{(0)}}\right) e^{i\varphi_i(t)}, \end{aligned} \tag{10}$$

where Eq. (5) was used in the second line. In the RWA, we can drop the oscillating entries of Eq. (9) and we arrive at the desired tripod Hamiltonian equation (1).

For negative detunings, i.e., $\omega > \varepsilon_i^{(0)}$, the direct coupling due to T_i and the indirect coupling due to L_i add up increasing the strength of the effective coupling. Depending on the ratio between the detuning and the energy gap, we have two different regimes. If $|\Delta_i^{(0)}| \ll \varepsilon_i^{(0)}$ we are in the small detuning regime and the second contribution dominates. If $|\Delta_i^{(0)}| \gg \varepsilon_i^{(0)}$, which is the case if the qubits energy splitting is much smaller than the cavity frequency, we are in the large detuning regime and the first contribution dominates. Theoretically, both regimes yield the tripod form of the effective Hamiltonian. Since the different regimes have different requirements on the experimental setup, which are readily available for small detuning regime, we study this in more detail below.

We used two approximations in the derivation of the tripod Hamiltonian. First, $g_i^{(0)} \ll \Delta_i^{(0)}$ was needed to derive Eq. (9). Although there exist higher order terms which might seem to destroy the ideal tripod structure, these can all be removed within the RWA. Nevertheless, there are higher order terms resulting in an effective coupling slightly lower than suggested by Eq. (10) and an optimal driving frequency marginally different from Eq. (8). Second, the RWA requires $L_i \ll \omega_i \approx \Delta_i^{(0)}$. Both relations limit the effective coupling strength of the indirect coupling, while the direct coupling is limited by $g_i^{(0)} \ll \varepsilon_i^{(0)}$ which was used to write down Eq. (2). To demonstrate a holonomy with current experimental limitations (decoherence times, qubit-cavity couplings, flux driving), one needs to reduce the detuning $\Delta_i^{(0)}$ to the edge of the validity of the above approximations. This is studied in Sec. IV.

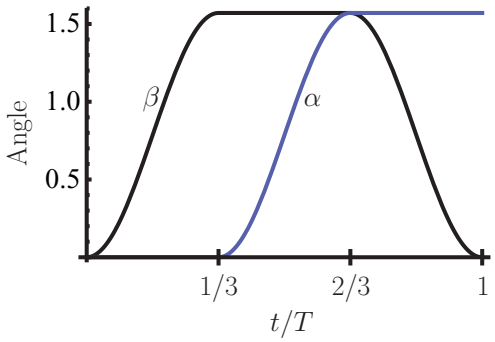

FIG. 2. (Color online) The parameters β (black) and α [blue (gray in the print version)] as a function of time during the adiabatic control cycle.

IV. RESULTS

In this section, we verify the validity of the above analytical results with numerical studies. As an example, we choose to work with a particular implementation of the non-Abelian operator proposed in Refs. 19 and 20 in which the Rabi frequencies Ω_i are real and parameterized as

$$\begin{aligned}\Omega_1 &= \Omega \sin\beta\cos\alpha,\\ \Omega_2 &= \Omega \sin\beta\sin\alpha,\\ \Omega_3 &= \Omega\cos\beta.\end{aligned} \tag{11}$$

Accordingly, in the driving fields in Eq. (6), we take $\varphi_i = 0$. We assume Ω to be constant, while the angles, α and β, change adiabatically in time.

Let us discuss some general properties of the tripod Hamiltonian in equation (1). It has two nondegenerate eigenstates, usually referred to as the bright states, with energies $\hbar\Omega = \pm\hbar\sqrt{\Omega_1^2+\Omega_2^2+\Omega_3^2}$ and, more importantly, a degenerate zero-energy subspace $\mathcal{E}(t) = \mathrm{span}\{|D_1(t)\rangle, |D_2(t)\rangle\}$. These so-called dark states are $|D_1(t)\rangle = \cos\beta(\cos\alpha|1\rangle + \sin\alpha|2\rangle) - \sin\beta|3\rangle$ and $|D_2(t)\rangle = \cos\alpha|2\rangle - \sin\alpha|1\rangle$. The system state $|\psi(0)\rangle$ is initially prepared to be in this subspace, and if the control parameters are changed adiabatically, then the system will stay in this subspace during the evolution. In particular, for a cyclic Hamiltonian $H(0) = H(T)$, the system will return to the initial subspace $\mathcal{E}(0)$. However, within this subspace, the state will undergo a nontrivial $U(2)$ transformation which is the holonomic operator.[28,29]

The evolution in the parameter space begins and ends at the point $(\Omega_1,\Omega_2,\Omega_3) = (0,0,\Omega)$ and by writing explicitly the dark states using Eq. (11), we obtain that the initial zero-energy subspace is spanned by $\{|1\rangle,|2\rangle\}$. These states are used as basis states of a logical qubit. An adiabatic change of the angles results in the holonomy[20]

$$U(\Sigma) = e^{i\Sigma\sigma_y}, \tag{12}$$

where Σ is the solid angle traces by (α,β) and σ_y is the Pauli matrix in the computational basis. In particular, the sequence

$$(\alpha(t),\beta(t)) : (0,0) \to (0,\pi/2) \to (\pi/2,\pi/2) \to (\pi/2,0), \tag{13}$$

results up to a phase factor in a holonomic NOT gate $U_{\mathrm{hol}} = |1\rangle\langle 2| - |2\rangle\langle 1|$ for the logical qubit. Note that because of the spherical parameterization, the Hamiltonian is cyclic. For better adiabaticity, we change the angles smoothly using sine functions and constants as shown in Fig. 2.

For a set of universal gates, a phase gate is also needed. According to Ref. 20, this is achieved in a similar manner by using complex Rabi frequencies Ω_i, which in turn results from changing the phase of the flux drive. For convenience, numerical studies of the phase gate are not presented here, as they resemble the ones presented here for the NOT gate.

To implement this loop in our setup, one can control the flux driving amplitudes $F_i(t)$ and hence the longitudinal driving amplitude $L_i(t)$ which is directly related to the Rabi frequencies by Eq. (10). The reference basis is given by Eq. (7) and the initial degenerate subspace corresponds to $|1\rangle \hat{=} v_1$ and $|2\rangle \hat{=} v_2$. In particular, we assume an initial state $|1\rangle$ and, for an ideal transformation, the final state is simply $|\psi_{\mathrm{ideal}}(T)\rangle = |2\rangle$. Thus, the fidelity, defined as $F(t) = |\langle\psi_{\mathrm{ideal}}(t)|\psi(t)\rangle|^2$, after the gate time T is the population of $|2\rangle$. For clarity, we only show the populations of $|1\rangle$ and $|2\rangle$ in Figs. 3 and 4. To evaluate the quality of the gate, we would have to check the fidelity for different initial conditions. However, because the validity of our approximations is independent of the initial state, their respective fidelities behave very similar and we do not show them explicitly.

We integrate the dynamics of the system using the ideal tripod Hamiltonian in Eq. (1) for different gate times T, as shown in Figs. 3(a) and 3(b). The fidelity is plotted over the gate time T in Fig. 3(c) which shows the expected approach to unity in the adiabatic limit. The slightly oscillatory behavior observed in Fig. 3(c) is typical for adiabatic gates.[30] However, one should not rely on local maxima of this curve, as their position depends on the precise value of several experimental parameters. Instead, one should use gate times long enough

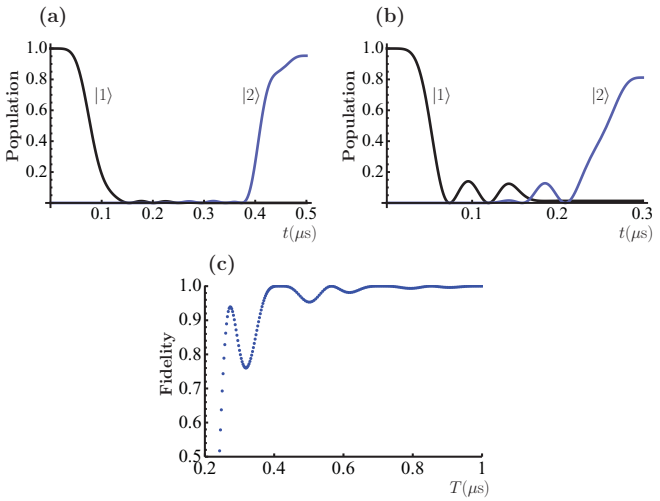

FIG. 3. (Color online) The population of the states $|1\rangle$ (black) and $|2\rangle$ [blue (gray in the print version)], obtained from the numerical integration of the Schrödinger equation using the effective Hamiltonian in Eq. (1) with $\Omega/2\pi = 10.5$ MHz. (a) The gate time $T = 0.5$ μs shows good population transfer, while (b) for $T = 0.3$ μs, the smaller fidelity indicates the invalidity of the adiabatic approximation. (c) The gate fidelity as a function of the gate time T.

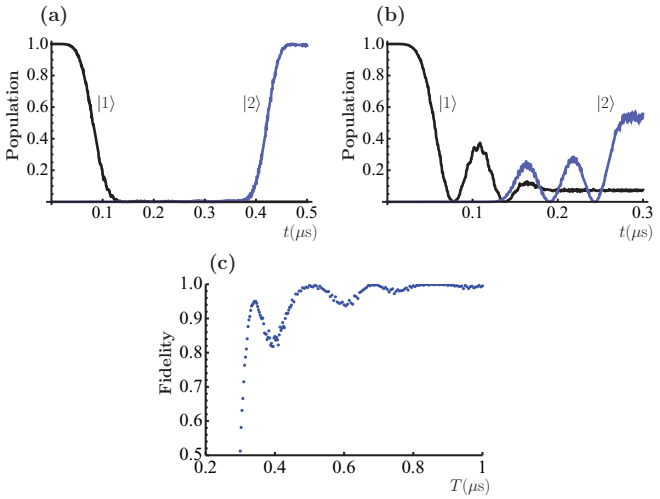

FIG. 4. (Color online) (a and b) The population of the states $|1\rangle$ (black) and $|2\rangle$ [blue (gray in the print version)], obtained from the numerical integration of the Schrödinger equation using the exact Hamiltonian equation (3). The parameters are as follows: $\omega/2\pi =$ 5 GHz, $g_1^{(0)}/2\pi = 60$ MHz, $g_2^{(0)}/2\pi = -80$ MHz, $g_3^{(0)}/2\pi =$ 100 MHz, $\Delta_1^{(0)}/2\pi = -300$ MHz, $\Delta_2^{(0)}/2\pi = -400$ MHz, and $\Delta_3^{(0)}/2\pi = -500$ MHz. The longitudinal driving has a restriction of $\max(L_i) = 100$ MHz, resulting in an effective coupling $\Omega/2\pi =$ 10.5 MHz. The gate times are $T = 0.5\ \mu$s in panel (a) and $T = 0.3\ \mu$s in panel (b). (c) The fidelity as a function of the gate time T.

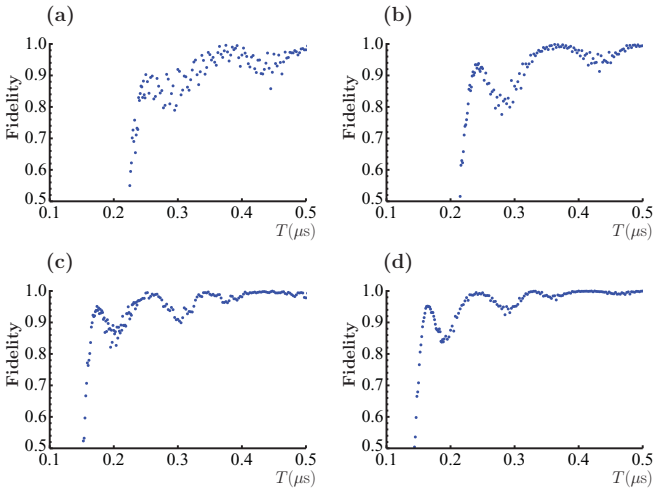

FIG. 5. (Color online) Gate fidelity as a function of gate time T. Parameters are chosen as in Fig. 4, but with stronger effective coupling achieved by using half the detuning $\Delta_i^{(0)}$ (a), double the qubit-cavity coupling $g_i^{(0)}$ (b), double the driving L_i (c), and double of all of them (d). This results in the effective couplings $\Omega/2\pi =$ 20.5 MHz (a), 21 MHz (b), 21 MHz (c), and 22 MHz (d).

such that even a local minimum provides a sufficiently good fidelity.

In Fig. 4, we integrate the exact Hamiltonian of Eq. (3). By comparing the results with Fig. 3, we can judge whether approximations such as the rotating wave approximation are satisfied. We use parameters which yield an effective coupling of $\Omega/2\pi = 10.5$ MHz (10 MHz, indirect coupling and 0.5 MHz, direct coupling). The results follow closely to the ones obtained by the effective tripod Hamiltonian, i.e., a gate time of 0.5 μs results in a fidelity of almost unity, whereas a gate time of 0.3 μs is not enough to justify the adiabatic approximation. The fidelity is plotted as a function of the gate time in Fig. 4(c), which shows much resemblance to the corresponding Fig. 3(c) except for a slight rescaling of the gate time. The reason for this rescaling is that $g_i^{(0)}/\Delta_i^{(0)} = 0.2$ is not small enough to perfectly justify the approximation $g_i^{(0)} \ll \Delta_i^{(0)}$, and therefore the formula [Eq. (10)] slightly overestimates the effective coupling as described in Sec. III

Because the decoherence time of transmons to date is of the order of a microsecond, one would wish to increase the effective coupling to achieve faster holonomies. This can be done in various ways as shown in Figs. 5(a)–5(d), always such that Eq. (10) suggests roughly double the effective coupling compared with Fig. 4(c). One would expect good fidelities in half the gate time compared with Fig. 4(c). The easiest and readily available way is to decrease the detunings Δ_i as shown in Fig. 5(a). However, the gate fidelity is by no means as good as expected from the effective coupling. The reason is that the conditions $L_i \ll \Delta_i^{(0)}$ and $g_i \ll \Delta_i^{(0)}$ used in the derivation of the effective Hamiltonian tend to get violated for decreasing $\Delta_i^{(0)}$. The situation is slightly better in Figs. 5(b) and 5(c), where the higher effective coupling is achieved by increasing the qubit-cavity coupling $g_i^{(0)}$ and the driving amplitude L_i, respectively. The only way to increase the effective coupling without affecting the validity of the approximations is to simultaneously increase $g_i^{(0)}$, L_i, and $\Delta_i^{(0)}$, which is shown in Fig. 5(d). However, it may be hard to achieve such high amplitudes L_i with current setups.

We would like to add a note on experimental feasibility. The parameters used in Fig. 4 are realistic in an existing experimental setup[2,31] and can be achieved [see Eq. (4)], for example, by using transmons with charging energy $E_C = 2\pi\hbar \times 280$ MHz, Josephson energy $E_{J\max} = 2\pi\hbar \times 224$ GHz, fluxes $\phi_1^{(0)} =$ 0.484 26, $\phi_2^{(0)} = 0.484\,89$, and $\phi_3^{(0)} = 0.485\,50$, and variations of the fluxes of up to $\max(\delta\phi_i) = 6.3 \times 10^{-4}$. To verify the geometric transformation, one has to be able to read out the final state of the system. For this purpose, one increases the detunings considerably such that the energy eigenstates v_i are approximate product states of the cavity and the three qubits. Then, it is sufficient to perform state tomography of the first and second qubits because the holonomy is a transformation between v_1 and v_2 only. State tomography has been demonstrated for up to three transmons in Refs. 32 and 33.

V. CONCLUSION

We proposed an experimental scheme for geometric non-Abelian single-qubit gates with superconducting qubits, which could serve as a first step toward geometric quantum computing. Although we did not explicitly take into account the decoherence in our studies, the gate time is within the decoherence time for current experimental setups allowing for proof of principle experiments. The detailed effects of decoherence can be studied along the lines of Refs. 34–36 and will be presented in a future publication. We note that

there could be considerable technical improvements in the near future concerning the decoherence time as well as the driving strength, leading to the possibility to carry out extensive small-scale quantum computing. We used the NOT gate as an example to calculate the gate fidelity, but the proposed scheme can be utilized to carry out any single-qubit transformation.[20]

ACKNOWLEDGMENTS

We would like to thank A. Abdumalikov, S. Filipp, M. Pechal, and A. Wallraff for fruitful discussions, in particular, with respect to experimental parameters. This work was funded by the EU FP7 GEOMDISS project. P.S. and M.M. acknowledge the Academy of Finland and Emil Aaltonen Foundation for financial support.

[1] Yu. Makhlin, G. Schön, and A. Shnirman, Rev. Mod. Phys. **73**, 357 (2001).

[2] J. M. Fink, R. Bianchetti, M. Baur, M. Göppl, L. Steffen, S. Filipp, P. J. Leek, A. Blais, and A. Wallraff, Phys. Rev. Lett. **103**, 083601 (2009).

[3] J. Koch, T. M. Yu, J. Gambetta, A. A. Houck, D. I. Schuster, J. Majer, A. Blais, M. H. Devoret, S. M. Girvin, and R. J. Schoelkopf, Phys. Rev. A **76**, 042319 (2007).

[4] A. Blais, R.-S. Huang, A. Wallraff, S. M. Girvin, and R. J. Schoelkopf, Phys. Rev. A **69**, 062320 (2004).

[5] A. Wallraff, D. I. Schuster, A. Blais, L. Frunzio, R.-S. Huang, J. Majer, S. Kumar, S. M. Girvin, and R. J. Schoelkopf, Nature **431**, 162 (2004).

[6] E. Knill, Nature **434**, 39 (2005).

[7] D. Gottesman, "Stabilizer Codes and Quantum Error Correction," Ph.D. thesis (California Institute of Technology, Pasadena, 1997).

[8] P. Zanardi and M. Rasetti, Phys. Lett. A **264**, 94 (1999).

[9] G. De Chiara and G. M. Palma, Phys. Rev. Lett. **91**, 090404 (2003).

[10] P. Solinas, P. Zanardi, and N. Zanghí, Phys. Rev. A **70**, 042316 (2004).

[11] P. J. Leek, J. M. Fink, A. Blais, R. Bianchetti, M. Göppl, J. M. Gambetta, D. I. Schuster, L. Frunzio, R. J. Schoelkopf, and A. Wallraff, Science **318**, 1889 (2007).

[12] M. Möttönen, J. J. Vartiainen, and J. P. Pekola, Phys. Rev. Lett. **100**, 177201 (2008).

[13] M.-S. Choi, J. Phys. Condens. Matter **15**, 7823 (2003).

[14] L. Faoro, J. Siewert, and R. Fazio, Phys. Rev. Lett. **90**, 028301 (2003).

[15] V. Brosco, R. Fazio, F. W. J. Hekking, and A. Joye, Phys. Rev. Lett. **100**, 027002 (2008).

[16] J.-M. Pirkkalainen, P. Solinas, J. P. Pekola, and M. Möttönen, Phys. Rev. B **81**, 174506 (2010).

[17] P. Solinas, J.-M. Pirkkalainen, and M. Möttönen, Phys. Rev. A **82**, 052304 (2010).

[18] J. Alicea, Y. Oreg, G. Refael, F. von Oppen, and M. P. A. Fisher, Nat. Phys. **7**, 412 (2011).

[19] R. G. Unanyan, B. W. Shore, and K. Bergmann, Phys. Rev. A **59**, 2910 (1999).

[20] L.-M. Duan, J. I. Cirac, and P. Zoller, Science **292**, 1695 (2001).

[21] I. Fuentes-Guridi, J. Pachos, S. Bose, V. Vedral, and S. Choi, Phys. Rev. A **66**, 022102 (2002).

[22] A. Recati, T. Calarco, P. Zanardi, J. I. Cirac, and P. Zoller, Phys. Rev. A **66**, 032309 (2002).

[23] P. Solinas, P. Zanardi, N. Zanghì, and F. Rossi, Phys. Rev. B **67**, 121307(R) (2003).

[24] P. Zhang, Z. D. Wang, J. D. Sun, and C. P. Sun, Phys. Rev. A **71**, 042301 (2005).

[25] J. A. Schreier, A. A. Houck, Jens Koch, D. I. Schuster, B. R. Johnson, J. M. Chow, J. M. Gambetta, J. Majer, L. Frunzio, M. H. Devoret *et al.*, Phys. Rev. B **77**, 180502(R) (2008).

[26] In fact, after cooling to the ground state, transversal driving is necessary for initialization in the one-excitation subspace. However, as this procedure is very much standard and can be performed with high fidelity it is not discussed further.

[27] There is a small correction $-E_C^{(i)}/\hbar$ to the energy splitting $\varepsilon_i(\phi_i)$. This correction does not depend on the flux and can therefore be disregarded, as it merely results in a shift of the detuning $\Delta_i^{(0)}$ which can be countered by adjusting the flux $\phi_i^{(0)}$.

[28] F. Wilczek and A. Zee, Phys. Rev. Lett. **52**, 2111 (1984).

[29] J. Anandan, Phys. Lett. A **133**, 171 (1988).

[30] G. Florio, P. Facchi, R. Fazio, V. Giovannetti, and S. Pascazio, Phys. Rev. A **73**, 022327 (2006).

[31] A. Abdumalikov, S. Filipp, M. Pechal, and A. Wallraff (private communication).

[32] S. Filipp, P. Maurer, P. J. Leek, M. Baur, R. Bianchetti, J. M. Fink, M. Göppl, L. Steffen, J. M. Gambetta, A. Blais, and A. Wallraff, Phys. Rev. Lett. **102**, 200402 (2009).

[33] L. DiCarlo, M. D. Reed, L. Sun, B. R. Johnson, J. M. Chow, J. M. Gambetta, L. Frunzio, S. M. Girvin, M. H. Devoret, and R. J. Schoelkopf, Nature **467**, 574 (2010).

[34] J. P. Pekola, V. Brosco, M. Möttönen, P. Solinas, and A. Shnirman, Phys. Rev. Lett. **105**, 030401 (2010).

[35] P. Solinas, M. Möttönen, J. Salmilehto, and J. P. Pekola, Phys. Rev. B **82**, 134517 (2010).

[36] J. Salmilehto, P. Solinas, J. Ankerhold, and M. Möttönen, Phys. Rev. A **82**, 062112 (2010).